Theoretical Analysis and Experimental Validation of Current Balancing in Parallel MHz WPT Systems with a Coupled Inductor Pair

Rintaro Kusui [1)] Taiga Osada [1)] Keisuke Kusaka [1)] Jun-ichi Itoh [1)]

1) Nagaoka University of Technology, Nagaoka, Niigata, Japan

E-mail: kusui@stn.nagaokaut.ac.jp

ABSTRACT: This paper presents a current balancing method utilizing a coupled inductor pair for a megahertz-band wireless power transfer (WPT) system, aiming to reduce the size and weight of transmission coils. In conventional systems, inverters are connected in parallel to enhance transmission power. However, it is crucial to mitigate circulating currents between the parallel-connected inverters to prevent thermal imbalance and potential damage. The proposed balancer equalizes the output currents of the inverters while suppressing common-mode currents. Its performance is evaluated through simulations and experiments. Simulation results for a 6.78 MHz WPT system demonstrate that the inverter output current aligns with the average current, with an error of only 0.17%. Furthermore, an experimental prototype operating at 85 kHz successfully transmits 2 kW of power while maintaining a current deviation of just 0.18% from the average.

KEYWORDS: wireless power transfer (WPT), coupled inductors, parallel inverters, current balancing

1. INTRODUCTION

Wireless power transfer (WPT) systems have been extensively studied for the convenient and safe charging of electric vehicles, drones, and other applications (1)(2). Among them, WPT systems operating in ISM bands such as 6.78 MHz and 13.56 MHz are particularly attractive due to their ability to reduce the size and weight of transmission coils (3)(4). However, the output power of megahertz-band inverters used in these systems is typically limited to a few kilowatts per unit, as gallium nitride (GaN) devices have constrained power dissipation due to their small chip size. To overcome this limitation, parallel connection of megahertz-band inverters has been proposed to increase transmission power (5)(6). However, in parallel-connected megahertz inverters, slight variations in output voltage can occur due to delays in driver ICs, switching devices, and wiring lengths. These voltage differences can cause circulating currents, leading to thermal imbalance and possible damage to the inverters. Therefore, ensuring balanced output currents among the inverters is essential.

Refs. (7) and (8) have proposed using coupled inductors to balance the currents in parallel inverter systems. In these methods, the parallel-connected current flows through the secondary winding of the coupled inductor, where the secondary-side current cancels the magnetic flux generated by the balanced current, allowing for a compact balancer design. However, these methods lack galvanic isolation, which can result in short-circuit currents if the inverters have different common-mode voltages.

This paper proposes a current balancer utilizing a coupled inductor pair for parallel-connected megahertz-band WPT systems. In the proposed system, a coupled inductor pair is inserted in series with each phase of the inverter. This configuration not only balances the inverter output currents but also suppresses high-frequency harmonics in the common-mode current by compensating for unbalanced voltage components. Additionally, the resonant capacitors of the WPT system are positioned between the balancer and the parallel connection point, providing high impedance to low-frequency and DC components of the common-mode current. When the magnetic coupling of coupled inductors is weak, a parallel-connected capacitor compensates for the leakage inductance.

The key contribution of this work is the development of a compact balancer that not only suppresses circulating currents but also offers sufficiently high impedance for common-mode voltages in each inverter. The effectiveness of the proposed approach is demonstrated through simulations at 6.78 MHz and experimental verification at 85 kHz.

2. PROPOSED SYSTEM

2.1. Proposed system configuration

Figure 1 shows the configuration of the proposed system. The proposed system is based on a series-series compensated WPT system, with resonant capacitors connected in series with the transmission coils. The resonant capacitors are connected between parallel connection points and the coupled inductors. These

capacitors provide high impedance to DC or low-frequency harmonic components of common mode voltage. A coupled inductor pair is connected in series with the lines of each inverter in the same current direction. The coupled inductors function as 0-degree 3 dB hybrids and balance the current. However, the low magnetic coupling of the coupled inductors causes the resonance frequency to drop due to leakage inductance. Figure 1(b) shows the system configuration when the leakage inductance is large. The parallel capacitor compensates for the leakage inductance because it operates as LCC compensation.

2.2. 0-degree 3dB hybrid by a coupled inductor pair

Figure 2 shows the circuit diagram of the 0-degree 3dB hybrid. The 3dB hybrid has two input ports and one output port. It combines the power from the two input ports and transmits it to the output port. Conversely, the 3dB hybrid distributes the power of the output port to the two input ports. The relationship between the input voltages v_1 and v_2, and the output voltage v_R is expressed as

$$v_R = \frac{v_1 + v_2}{2} \quad \cdots\cdots (1).$$

No power is transmitted due to the very high impedance between the input ports of an ideal hybrid. Thus, the input currents i_1 and i_2 are equal. Accordingly, the relationship between output port current i_R and input port currents i_1 and i_2 is expressed as

$$i_R = i_1 + i_2 = 2i_1 = 2i_2 \quad \cdots\cdots (2).$$

Therefore, the 3dB hybrid also works as a current balancer.

2.3. Current analysis and design of the coupled inductor pair with strong coupling

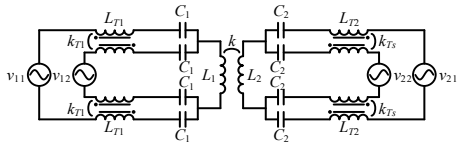

(a) Coupled inductor with strong coupling

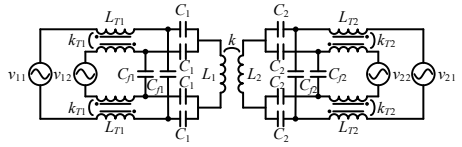

(b) Coupled inductor with weak coupling and compensation capacitors

Fig. 1. Proposed WPT system.

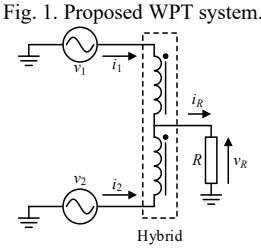

Fig. 2. Configuration of 0-degree 3dB hybrid.

The circuit equation of the proposed system without parallel capapcitors is given by (3), where L_{Tn} is the self-inductance of the balancer, k_{Tn} is the coupling coefficience, V_{nm} is the primary or secondary converter output voltage, L_n is the self-inductance of the transmission coils, and C_n is the resonant capacitors (n, m = 1, 2). Resonance frequency ω is expressed as

$$\omega = \frac{1}{\sqrt{L_1 C_1}} = \frac{1}{\sqrt{L_2 C_2}} \quad \cdots\cdots (4).$$

The converter currents I_{11}, I_{12}, I_{21}, and I_{22} are derived from (3) under resonance conditions and are given by (5). The first and second terms in (5) represent the balanced component of the converter current, whereas the third term corresponds to the circulating current component. Specifically, the first term 8contributes to the power transfer, while the second term

$$\begin{pmatrix} V_{11} \\ V_{12} \\ V_{21} \\ V_{22} \end{pmatrix} = \begin{pmatrix} j2\omega L_{T1} + \dfrac{2}{j\omega C_1} + j\omega L_1 & j\omega L_1 - j2\omega k_{T1} L_{T1} & j\omega M & j\omega M \\ j\omega L_1 - j2\omega k_{T1} L_{T1} & j2\omega L_{T1} + \dfrac{2}{j\omega C_1} + j\omega L_1 & j\omega M & j\omega M \\ j\omega M & j\omega M & j2\omega L_{T2} + \dfrac{2}{j\omega C_2} + j\omega L_2 & j\omega L_2 - j2\omega k_{T2} L_{T2} \\ j\omega M & j\omega M & j\omega L_2 - j2\omega k_{T2} L_{T2} & j2\omega L_{T2} + \dfrac{2}{j\omega C_2} + j\omega L_2 \end{pmatrix} \begin{pmatrix} I_{11} \\ I_{12} \\ I_{21} \\ I_{22} \end{pmatrix} \cdots (3).$$

$$\begin{pmatrix} I_{11} \\ I_{12} \\ I_{21} \\ I_{22} \end{pmatrix} = \begin{pmatrix} \dfrac{j\omega M (V_{21} + V_{22})}{4\omega^2 \left((1-k_{T1})(1-k_{T2}) L_{T1} L_{T2} - M^2\right)} \\ \dfrac{j\omega M (V_{21} + V_{22})}{4\omega^2 \left((1-k_{T1})(1-k_{T2}) L_{T1} L_{T2} - M^2\right)} \\ \dfrac{j\omega M (V_{11} + V_{12})}{4\omega^2 \left((1-k_{T1})(1-k_{T2}) L_{T1} L_{T2} - M^2\right)} \\ \dfrac{j\omega M (V_{11} + V_{12})}{4\omega^2 \left((1-k_{T1})(1-k_{T2}) L_{T1} L_{T2} - M^2\right)} \end{pmatrix} - \begin{pmatrix} \dfrac{j\omega (1-k_{T2}) L_{T2} (V_{11} + V_{12})}{4\omega^2 \left((1-k_{T1})(1-k_{T2}) L_{T1} L_{T2} - M^2\right)} \\ \dfrac{j\omega (1-k_{T2}) L_{T2} (V_{11} + V_{12})}{4\omega^2 \left((1-k_{T1})(1-k_{T2}) L_{T1} L_{T2} - M^2\right)} \\ \dfrac{j\omega (1-k_{T1}) L_{T1} (V_{21} + V_{22})}{4\omega^2 \left((1-k_{T1})(1-k_{T2}) L_{T1} L_{T2} - M^2\right)} \\ \dfrac{j\omega (1-k_{T1}) L_{T1} (V_{21} + V_{22})}{4\omega^2 \left((1-k_{T1})(1-k_{T2}) L_{T1} L_{T2} - M^2\right)} \end{pmatrix} + \begin{pmatrix} -\dfrac{V_{11} - V_{12}}{j4\omega \left((1+k_{T1}) L_{T1} - L_1\right)} \\ \dfrac{V_{11} - V_{12}}{j4\omega \left((1+k_{T1}) L_{T1} - L_1\right)} \\ -\dfrac{V_{21} - V_{22}}{j4\omega \left((1+k_{T2}) L_{T2} - L_2\right)} \\ \dfrac{V_{21} - V_{22}}{j4\omega \left((1+k_{T2}) L_{T2} - L_2\right)} \end{pmatrix} \cdots (5).$$

represents the reactive current, which does not contribute to the power transfer. Eq. (5) indicates that a sufficiently strong balancer coupling coefficient can eliminate the reactive current and effectively suppress the circulating current.

The circulating current is defined as the difference between the inverter currents I_{n1} and I_{n2} (n = 1, 2) and is expressed as (6) assuming that the balancer coupling is sufficiently strong.

$$I_{n1} - I_{n2} = -\frac{V_{n1} - V_{n2}}{j2\omega\left(L_n - 2L_{Tn}\right)} \quad \cdots\cdots (6).$$

The ratio of the difference between the output voltage of the inverter and the circulating current determines the suppression effect of the circulating current in the proposed balancer. Accordingly, the circulating current suppression effect $|Z_{dn}|$ is given by

$$\left|Z_{dn}\right| = \left|\frac{V_{n1} - V_{n2}}{I_{n1} - I_{n2}}\right| = 2\omega\left(2L_{Tn} - L_n\right) \quad \cdots\cdots (7).$$

Thus, the self-inductance L_{T1} of the coupled inductors is designed using (8) based on suppression effect $|Z_{dn}|$ of the circulating current.

$$L_{Tn} \geq \frac{\left|Z_{dn}\right|}{4\omega} + \frac{L_n}{2} \quad \cdots\cdots (8).$$

2.4. Current analysis and design of the coupled inductor pair with low coupling

Coupling inductors in high frequency WPT systems consist of either an air core or a low permeability dust core. The coupling coefficient can drop to about 0.8 with low permeability core materials. Leakage inductance reduces the power factor of the inverter and the transmitted power. Parallel capacitors compensate for this leakage inductance as shown in figure 2(b). The parallel capacitance is designed based on the LCC compensation method. The resonance condition of LCC compensation is expressed as

$$\omega = \frac{1}{\sqrt{2\left(1-k_{Tn}\right)L_{Tn}C_{fn}}} = \frac{1}{\sqrt{2L_1\dfrac{C_nC_{fn}}{C_n + 2C_{fn}}}} \qquad \left(n = 1, 2\right) \quad \cdots (9).$$

The converter currents I_{11}, I_{12}, I_{21}, and I_{22} are derived as (10) from the schematic in figure 1 (b). The first term in (10) shows the symmetrical component of the drive current and indicates that there is no reactive current. Since the circulating current is the difference between the drive currents, it is expressed as twice the second term in (10). Accordingly, the effect of the balancer on the suppression of the circulating current is expressed as

$$\begin{pmatrix} I_{11} \\ I_{12} \\ I_{21} \\ I_{22} \end{pmatrix} = \begin{pmatrix} \dfrac{j\omega M\left(V_{21}+V_{22}\right)}{4\omega^2\left(1-k_{T1}\right)\left(1-k_{T2}\right)L_{T1}L_{T2}} \\ \dfrac{j\omega M\left(V_{21}+V_{22}\right)}{4\omega^2\left(1-k_{T1}\right)\left(1-k_{T2}\right)L_{T1}L_{T2}} \\ \dfrac{j\omega M\left(V_{11}+V_{12}\right)}{4\omega^2\left(1-k_{T1}\right)\left(1-k_{T2}\right)L_{T1}L_{T2}} \\ \dfrac{j\omega M\left(V_{11}+V_{12}\right)}{4\omega^2\left(1-k_{T1}\right)\left(1-k_{T2}\right)L_{T1}L_{T2}} \end{pmatrix} + \begin{pmatrix} -\dfrac{j\omega L_1\left(V_{11}-V_{12}\right)}{4\omega^2 L_{T1}\left(\left(1-k_{T1}\right)^2 L_{T1} + 2k_{T1}L_1\right)} \\ \dfrac{j\omega L_1\left(V_{11}-V_{12}\right)}{4\omega^2 L_{T1}\left(\left(1-k_{T1}\right)^2 L_{T1} + 2k_{T1}L_1\right)} \\ -\dfrac{j\omega L_1\left(V_{21}-V_{22}\right)}{4\omega^2 L_{T2}\left(\left(1-k_{T2}\right)^2 L_{T2} + 2k_{T2}L_2\right)} \\ \dfrac{j\omega L_1\left(V_{21}-V_{22}\right)}{4\omega^2 L_{T2}\left(\left(1-k_{T2}\right)^2 L_{T2} + 2k_{T2}L_2\right)} \end{pmatrix} \quad \cdots\cdots (10)$$

Table 1. Simulation condition

Prameters	Symbol	Value
DC voltage	V_{DC1}, V_{DC2}	200 V
Rated output power	P_{out}	2 kW
Transmission frequency	f	6.78 MHz
Transmission coil	L_1, L_2	1.90 μH
Coupling coefficient	k	0.2 -
Balancer at k_T = 1	L_{T1}, L_{T2}	6.82 μH
Balancer at k_T = 0.9388		6.21 μH
Compensation capacitors	C_{p1}, C_{p2}	725 pF
Resonance capacitors at k_T = 1	C_1, C_2	289 pF
Resonance capacitors at k_T = 0.9388		362 pF

$$\left|Z_{dn}\right| = \left|\frac{V_{n1} - V_{n2}}{I_{n1} - I_{n2}}\right| = 2\omega\frac{L_{Tn}}{L_n}\left(\left(1-k_{Tn}\right)^2 L_{Tn} + 2k_{Tn}L_n\right) \quad \cdots\cdots (11).$$

From (11), the self-inductance of the balancer with parallel capacitors is designed by (12) based on suppression effect $|Z_{dn}|$ of the circulating current.

$$L_{Tn} = \sqrt{\frac{k_{Tn}^2 L_n^2}{\left(1-k_{Tn}\right)^4} + \frac{\left|Z_{dn}\right|L_n}{2\omega\left(1-k_{Tn}\right)^2}} - \frac{k_{Tn}}{\left(1-k_{Tn}\right)^2}L_n \quad \cdots\cdots (12).$$

3. SIMULATION RESULTS

Figure 3 shows the simulation results of the proposed system when the magnetic coupling of the balancer is strong enough, and Table 1 shows the simulation conditions. The transmission frequency is 6.78 MHz, the transmission power is 2 kW and the output power of the inverter is 1 kW. The self-inductance of the balancer is 6.82 μH when the circulating current suppression effect $|Z_d|$ is 20dB (1 kΩ). Figure 3(a) shows the operating waveform with the balancing output voltage of the inverter, and Figure 3(b) shows the waveform with the delay on Inv. 2. The delay between the two inverters is 8.2 ns (20 degrees), which includes the length of the switching elements, gate drivers and signal lines. Figure 3(a) shows that the two inverters output 1 kW at a power factor of 1. The output of Inv.1 and Inv.2 is 5.61 Arms. Figure 3(b) shows that

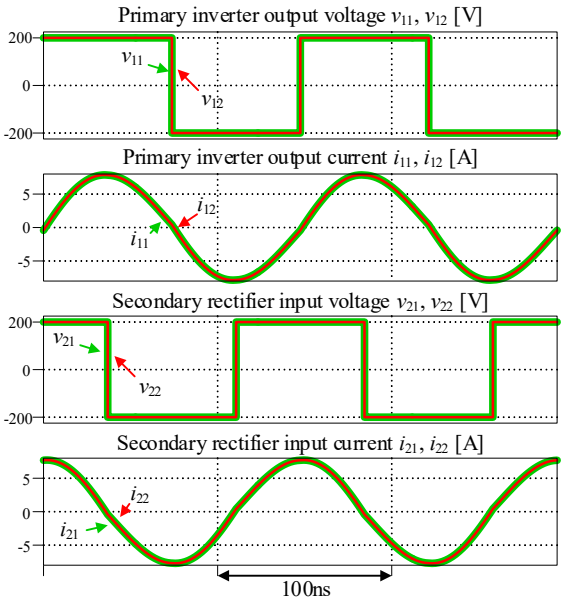

(a) Without phase difference between two inverters

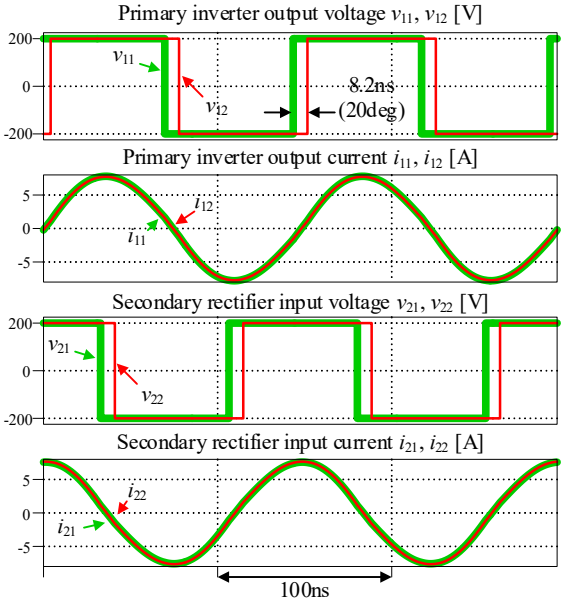

(b) With 8.2 ns delay between two inverters

Fig. 3. Simulation result of proposed system at coupling coefficient of 1.

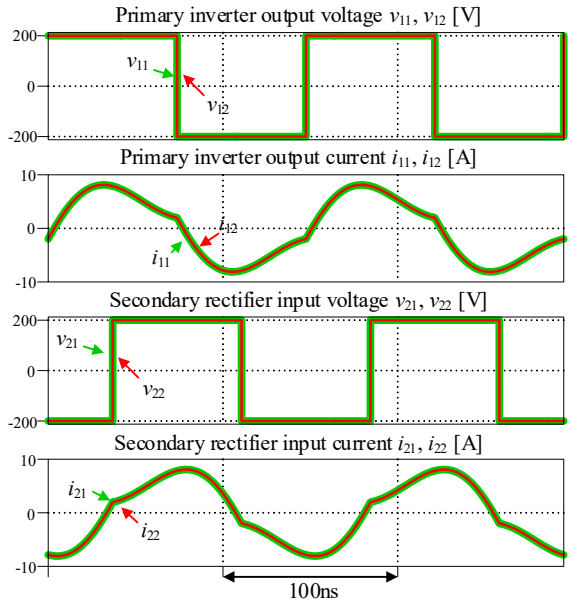

(a) Without phase difference between two inverters

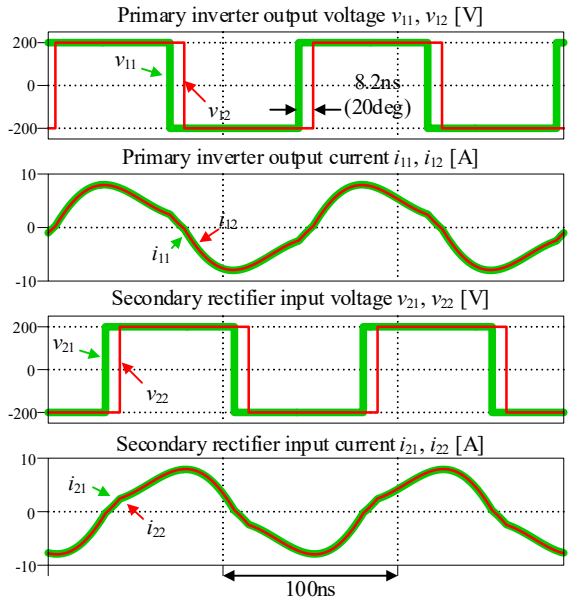

(b) With 8.2 ns delay between two inverters

Fig. 4. Simulation result of proposed system at coupling coefficient of 0.9388.

the output power of the inverters is 984 W. The phase difference in the inverter voltage reduces the transmitted power because the balancer reduces the power factor to compensate for the unbalance in the inverter output voltage. The output currents of the primary side inverters are 5.55 A and 5.38 A. Meanwhile, the input currents of the secondary rectifiers are 5.38 A and 5.45 A. In addition, the ratio of the inverter voltage difference to the fundamental component of the circulating current is 1000. The simulation results confirm the designed effect of suppressing the circulating current.

Figure 4 shows the operating waveform when the coupling coefficient of the balancer is 0.9388. The self-inductance of the balancer is 6.21 μH, the parallel capacitance is 725 pF, respectively, when the circulating current suppression effect $|Z_d|$ is 20dB (1kW). Figure 4(a) shows the operating waveform of the inverter output voltage without phase difference, and Figure 4(b) shows the waveform of the voltage with a phase difference of 20 degrees. Figure 4 shows that the inverter operates with a power factor of 1 due to the parallel capacitor. The inverter currents are the same when there is no phase difference in the inverter voltage. On the other hand, the output currents of the primary inverter are 5.56 A and 5.50 A and the input currents of the secondary rectifier are 5.47 A and 5.53 A when there is a phase difference. The ratio of the inverter voltage difference to the fundamental component of the circulating current is 1000. Thus, the simulation results confirm the designed effect of suppressing the circulating current.

4. EXPERIMENTAL RESULTS

Table 1 presents the experimental conditions. The proposed system is tested at 85 kHz for simplicity. The self-inductance of the coupled inductor is 603 μH and the coupling coefficient is 0.99.

Figure 5 shows the operating waveforms when there is no phase difference in the inverter output voltages. The waveforms show the output voltages of Inv. 1 and Rec. 1, as well as the currents in the transmission coils. The WPT system operates under resonance conditions because the power factor is approximately unity and the phase difference between the primary and secondary currents is nearly 90 degrees. The transmission power is 2.26 kW.

Figure 6 shows the operating waveforms when the phase difference in the inverter output voltages is 654 ns (20 degrees). Figure 6(a) shows the output voltages of Inv. 1 and Rec. 1, as well as the currents in the primary and secondary coils, while Figure 6(b) shows the output voltages and currents of Inv. 1 and Inv. 2, along with the calculated circulating current. The results show that the transmission power is 2.20 kW and the output current of Inv. 1 and Inv. 2 are 5.68A and 5.69A, respectively. The error from the average current is 0.18%. Fig. 6 (a) shows that the primary side power factor is deteriorating because the balancer compensates for the unbalanced voltage to balance the currents.

5. CONCLUSIONS

This paper proposed a current balancer using a coupled inductor pair for parallel-connected megahertz-band WPT systems. The inductance of the coupled inductors was designed based on the ratio of the inverter output voltage to the circulating current. The proposed system was evaluated through simulations and an experimental prototype operating at 85 kHz. The results confirmed that the circulating current was effectively reduced to nearly zero while achieving a power transmission of 2 kW.

Future work will focus on experimental validation in a megahertz-band WPT system to further assess the performance of the proposed method.

Table 2. Experimental condition

Prameters	Symbol	Value
DC voltage	V_{DC1}, V_{DC2}	200 V
Rated output power	P_{out}	2 kW
Transmission frequency	f	85 kHz
Transmission coil	L_1, L_2	151 μH
Coupling coefficient	k	0.2 -
Resonance capacitors	C_1, C_2	23.1 nF
balancer	L_{T1}, L_{T2}	603 μH

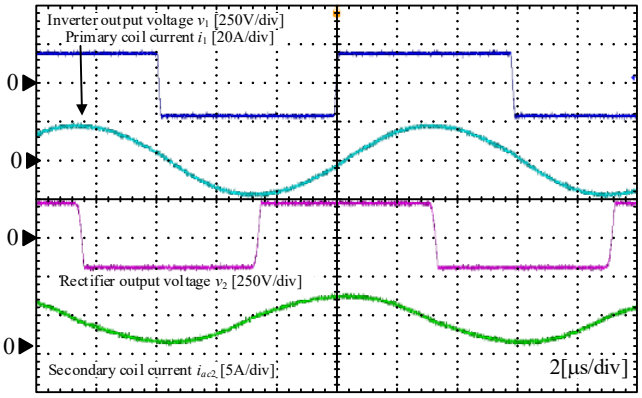

Fig. 5. Operation waveform of proposed system without phase difference in inverter output voltages.

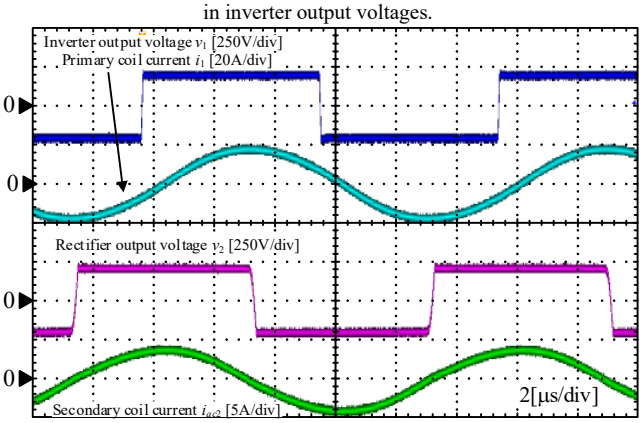

(a) Inverter and rectifier output voltages and coil currents

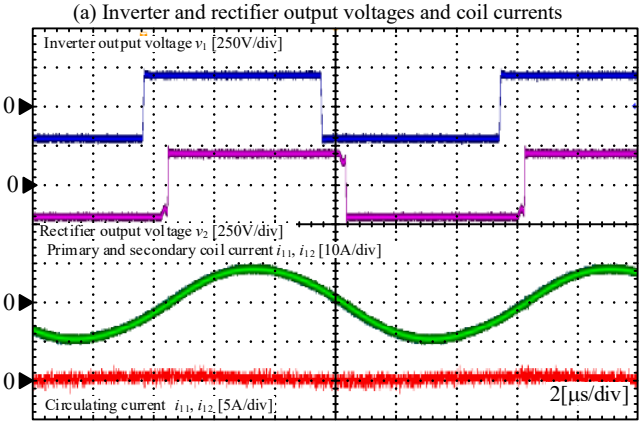

(b) Inverter output voltages and currents

Fig. 6. Operation waveform of proposed system with 654 ns (20 deg) phase difference in inverter output voltages.

REFERENCES

J. Li and D. Costinett, "Comprehensive Design for 6.78 MHz Wireless Power Transfer Systems", 2018 IEEE Energy Conversion Congress and Exposition (ECCE), 2018, pp. 906-913.

(2) N. K. Trung, T. Ogata, S. Tanaka and K. Akatsu, "Attenuate Influence of Parasitic Elements in 13.56-MHz Inverter for Wireless Power Transfer Systems," in IEEE Trans. on Power Electronics, vol. 33, no. 4, pp. 3218-3231, April 2018.

(3) N. K. Trung, T. Ogata, S. Tanaka, K. Akatsu, “Analysis and PCB Design of Class D Inverter for Wireless Power Transfer

Systems Operating at 13.56MHz", IEEJ Journal of Industry Applications, 2015, vol 4, no.6, pp. 703-713.

(4) S. Suzuki, T. Shimizu, "A Study on Efficiency Improvement of High-frequency Current Output Inverter Based on Immittance Conversion Element", IEEJ Journal of Industry Applications, 2015, vol 4, no.3, pp. 220-226.

(5) J. Shi, L. Zhou and X. He, "Common-Duty-Ratio Control of Input-Parallel Output-Parallel (IPOP) Connected DC–DC Converter Modules With Automatic Sharing of Currents," in IEEE Trans. on Power Electronics, vol. 27, no. 7, pp. 3277-3291, July 2012

(6) N. K. Trung and K. Akatsu, "Design challenges for 13.56MHz 10 kW resonant inverter for wireless power transfer systems", 2019 10th International Conference on Power Electronics and ECCE Asia (ICPE 2019 – ECCE Asia), Busan, Korea (South), 2019, pp. 1-7.

(7) S. Suzuki, S. Ogasawara, K. Orikawa, Miniaturization and Current Detection of Coupled-Inductor Circuit for Reducing Cross Currents of Modular Paralleled Power Converters, IEEJ Trans. on Industry Applications, 2023, Volume 143, Issue 3, Pages 177-186

(8) M. Yamaguchi, K. Kusaka and J. Itoh, "Current Balancing Method in Parallel Connected Inverter Circuit for Megahertz WPT System," 2021 IEEE 30th International Symposium on Industrial Electronics (ISIE), 2021, pp. 1-6